A Nonlinear Observer for Rotor Flux Estimation of Induction Motor Considering the Estimated Magnetization Characteristic

Francesco Alonge, *Member, IEEE*, Maurizio Cirrincione, *Senior Member, IEEE*, Marcello Pucci, *Senior Member, IEEE*, and Antonino Sferlazza, *Member, IEEE*

***Abstract*—This paper proposes a nonlinear observer for induction machine drives based on space-vector dynamic model of induction machine, expressed in state form, which presents the peculiarity of taking into consideration the magnetic saturation of the iron core. This observer is particularly suitable in order to obtain high accuracy in rotor flux estimation, in both amplitude and phase position, during working conditions characterized by varying flux, among which the most important are those during electrical losses minimization. A Lyapunov-based convergence analysis is proposed in order to suitably compute the numerical observer gain guaranteeing the convergence of the estimation error. The proposed nonlinear observer has been tested by means of simulations and experiments carried out on a suitably developed test setup. Its behavior has been compared with that obtained with a standard full-order Luenberger observer that assumes the linearity of the magnetization characteristic. The paper shows the capability of the proposed nonlinear observer to correctly estimate amplitude and phase of the rotor flux under flux varying conditions. Moreover, the proposed observer exhibits a higher accuracy than that obtained with the standard observer, which does not consider the estimated magnetization characteristic.**

***Index Terms*—Saturation, induction motor, magnetic, minimum-losses/maximum-efficiency, nonlinear observer.**

I. Introduction

CONTROL of induction machine (IM) has been a challenging research subject for many years. Starting from scalar control solution based on the steady-state model of the IM, the industrial standard in terms of high performance control of IMs it has been established as the so-called field oriented control [1]–[3]. As is well known, direct field oriented control requires the correct knowledge of the amplitude and phase of the flux space-vector. This is generally performed adopting suitably developed observers based on the dynamic equations of the IM, expressed in terms of the flux components. There are basically two forms of implementation of an observer: open loop and closed loop. The distinction between the two is whether or not a correction term, involving an estimation error, is exploited to adjust online the response of the observer [1]. In general, closed-loop observers are preferable to open-loop ones, since they permit the robustness against parameter variations and model errors to be improved. If a deterministic plant for the machine is considered, correspondingly the observer is a deterministic observer, such as the full-order Luenberger observer (FOLO) [4], [5] and the reduced order observer [6], [7]. On the contrary, if a stochastic model for the machine is considered, the Kalman filter (KF) can be used, respectively, in its linear or nonlinear version [extended KF (EKF)] [8], [9]. Another approach for the analysis of the observer has been proposed in [10], integrated with a detailed sensitivity analysis versus the parameters variations [11]. Finally, in [12] and recently in [13], analysis of flux observers are proposed from a perspective of the control system theory. Apart from the EKF, whose complexity and computational requirement is high besides the difficulty of its tuning, all the above observers are linear time-varying (not considering the speed as a state variable, but as a parameter).

There are, however, working conditions where contemporary speed and rotor flux variations occur, as for example in case of adoption of techniques for the online electric losses minimization. In such conditions, the conventional IM state-space model, which assumes a linear magnetic characteristic, does not provide a good accuracy in the estimation of the amplitude and phase position of the flux space-vector. In such working conditions the dynamic model of the IM vary consistently, with the inductance and leakage factors that vary with the magnetization level of the machine with nonlinear laws; new nonlinear terms arise. To properly deal with the nonlinearity of iron core, a specific model must be developed. Such model, to be suitably used for designing a flux observer, must be then expressed in state form. Some dynamic models of IM taking into consideration the magnetization characteristic have been developed in the scien-

Manuscript received October 4, 2016; revised January 30, 2017 and April 11, 2017; accepted May 25, 2017. Date of publication May 31, 2017; date of current version November 20, 2017. Paper 2016-IACC-0973.R2, presented at the 2015 Energy Conversion Congress and Exposition, Montreal, QC, Canada, Sep. 20–24, and approved for publication in the IEEE Transactions on Industry Applications by the Industrial Automation and Control Committee of the IEEE Industry Applications Society. This work was supported by RITmare, Italian Research for the Sea, under Grant CUP: B91J11000740001. *(Corresponding author: Marcello Pucci.)*

F. Alonge and A. Sferlazza are with the Department of Energy Information Engineering and Mathematical Models (D.E.I.M.), University of Palermo, Palermo 90128, Italy (e-mail: francesco.alonge@unipa.it; antonino.sferlazza@unipa.it).

M. Cirrincione is with the School of Engineering, University of the South Pacific, Laucala Campus, Suva 0679, Fiji Islands (e-mail: m.cirrincione@ieee.org).

M. Pucci is with I.S.S.I.A. of the National Research Council of Italy (CNR), Section of Palermo (Institute on Intelligent Systems for Automation), Palermo 90128, Italy (e-mail: pucci@pa.issia.cnr.it).

Color versions of one or more of the figures in this paper are available online at http://ieeexplore.ieee.org.

Digital Object Identifier 10.1109/TIA.2017.2710940

0093-9994 © 2017 IEEE. Personal use is permitted, but republication/redistribution requires IEEE permission.
See http://www.ieee.org/publications_standards/publications/rights/index.html for more information.

tific literature [14]–[17], each of which presents its peculiarity in representing the magnetizing characteristics.

As for the state observers, traditional observers are widely adopted for flux estimation of IMs and they work well in traditional constant flux working conditions. For such applications, observers are tuned assuming the values of the electrical parameters, in particular inductances and leakage factors, corresponding to unique working point on the knee of the magnetic characteristic. When the drive is required, however, to work in variable flux working conditions, as it is the case of adoption of any electrical losses minimization technique, the working point changes on the magnetic characteristic according to the speed and the load, and correspondingly also the electrical parameters of the machine vary and even its dynamics is modified. In variable working conditions, it is still possible to adopt traditional observers to estimate the flux, but the accuracy in the estimation of the magnitude and phase positions is expected to deteriorate. An observer accounting for the nonlinearities arising from considering the magnetic saturation of the iron core permits, on the contrary, a far better accuracy in flux estimation. The design of such a nonlinear observer with gains ensuring theoretically the stability is not, however, a trivial and well-defined problem. Moreover the use of an accurate flux estimation is necessary when high performance model-based control techniques are used [18], [19], since an inaccurate flux estimation of the machine under control can make the performance of the system be even worse than those achievable with other less sophisticated techniques.

The scientific literature offers several methods for designing and tuning nonlinear observers, all which present the hypothesis of a guaranteed convergence of the observer (convergence to zero of the estimation error) [20]–[22]. If nonlinear systems are considered, neither the observer structure nor the gain choice is straightforward as is typically in the case of linear systems: Very interesting design tools have been presented for the correct design of nonlinear observers. To the best knowledge of the authors, none of these observers have been applied to the IM flux estimation taking into consideration the magnetization characteristic.

Starting from the above considerations, this paper proposes a nonlinear observer for IM drives that takes into consideration the nonlinearity of the iron core as in [23], which is a preliminary version of this paper. The nonlinear observer is based on an original formulation of the dynamic model of the IM including the magnetization characteristic, which is inspired to [1, Ch. 6], but entirely reformulated, rearranging it in state-space form, after assuming as state variables, the stator current, and the rotor magnetizing current space-vectors. Moreover, the dynamic model of the IM has been expressed in the stator reference frame differently from [1]. Obviously, the magnetization characteristic is unknown and consequently it has been previously offline estimated starting from input–output experimental data. Moreover, it is also shown a way to express analytically the parameters of the model together with the magnetic characteristic, allowing to prove the above illustrated results; finally, it permits the gains of the observer to be expressed in a closed form with a direct and simple setup and implementation of the observer.

The convergence of the estimation error has been proved by means of a Lyapunov approach, and arbitrary global uniform exponential bounds have been imposed on the estimation error, regardless of the rotor speed. Moreover, it is shown that no bound neither on the rotor speed nor on the magnetizing current is required for the convergence of the estimation error. This aspect is particular important during the design phase of an observer, because the designer, besides ensuring the convergence of the estimated variables in each operating condition, can choose the speed of convergence, and can find, *a priori*, the correct tradeoff between filtering action and speed of convergence in a systematic way.

The proposed nonlinear observer has been tested in numerical simulations and experimentally on a suitably developed test setup. Its behavior has been compared to that of a classic FOLO, not taking into consideration the nonlinear magnetization characteristic, in variable flux working conditions.

Notation:

1) $\boldsymbol{A}\otimes\boldsymbol{B}$ denotes the Kronecker product between $\boldsymbol{A}$ and $\boldsymbol{B}$.
2) Given a square matrix $\boldsymbol{A}$ with real elements, it is defined $\mathrm{He}\{\boldsymbol{A}\} = \boldsymbol{A} + \boldsymbol{A}^T$.
3) $\boldsymbol{I}_2 = \begin{bmatrix} 1 & 0 \\ 0 & 1 \end{bmatrix}$, $\boldsymbol{J}_2 = \begin{bmatrix} 0 & -1 \\ 1 & 0 \end{bmatrix}$.

II. Space-Vector Dynamic Model of IM Considering the Magnetic Saturation

Among the different dynamic models of the IM taking into consideration the saturation of the iron core, as proposed in the scientific literature, the most of them are expressed in the field oriented reference frame [1] and [17]. A different approach has been followed in this paper, where the adopted model has been expressed in the stator reference frame. Such a choice implies that the knowledge of the angular position of the rotor magnetizing current space-vector is not needed. Such model, expressed in this form, reveals quite complex since it contains, with respect to the classic dynamic model of the IM, additional nonlinear terms as well as the nonlinear mapping representing the variations of both the inductance and leakage factor terms with respect to the amplitude of the rotor magnetizing current. On the contrary, it reveals particularly suitable for the development of a full-order nonlinear observer. One of the simplifying assumption of the proposed model is that the leakage inductances $L_{\sigma r}$ and $L_{\sigma s}$ are assumed to be constant and, therefore, not depending on the magnetizing flux. This is the common assumption of the model proposed in [1], reformulated here in state form to be adopted for designing the nonlinear state observer. Such an assumption corresponds to neglect the effect of the load on the saturation, which is a peculiarity of this model and represents a secondary aspect to be modeled as far as the magnetic saturation is concerned. Recently developed models, [24], [25], are able to consider the effect of the load on the magnetic saturation; such models, however, besides the much higher complexity and computational demand, are very hardly writable in state-space form as required for designing a state observer. On the basis of the above considerations, the dynamic model provided in [1, Sec. 6.1.1.1] can be elaborated in order to obtain a full-state

TABLE I
LIST OF SYMBOLS

SYMBOLS	
u_{sD}, u_{sQ}	Stator voltages in stator reference frame.
i_{sD}, i_{sQ}	Stator currents in stator reference frame.
i_{sx}, i_{sy}	Stator currents in rotor flux reference frame.
i_{mrd}, i_{mrq}	Rotor magnetizing currents in stator reference frame.
$\lvert\boldsymbol{\Psi}_r\rvert = L_m \lvert\boldsymbol{i}_{mr}\rvert$.	Rotor flux amplitude.
$L_s\,(L_r)$	Stator (rotor) inductance.
L_m	Three-phase magnetizing inductance.
$R_s\,(R_r)$	Stator (rotor) resistance.
$L_{s\sigma}\,(L_{r\sigma})$	Stator (rotor) leakage inductance.
$\sigma = 1 - \frac{L_m^2}{L_s L_r}$.	Global leakage factor.
$T_r = \frac{L_r}{R_r}$.	Rotor time constant.
ω_r	Angular speed of the rotor (in electrical angles).
p	Number of pole pairs.

representation expressed in the stator reference frame

$$\begin{cases} \dot{\boldsymbol{x}} = \boldsymbol{A}(|\boldsymbol{i}_{mr}|, \omega_r)\boldsymbol{x} + \boldsymbol{f}(\boldsymbol{x}) + \boldsymbol{G}\boldsymbol{u} \\ \boldsymbol{y} = \boldsymbol{C}\boldsymbol{x} \end{cases} \tag{1}$$

where $\boldsymbol{x}$ is the state vector, $\boldsymbol{u}$ is the input vector, and $\boldsymbol{y}$ is output vector, defined as

$$\begin{aligned} \boldsymbol{x} &= \begin{bmatrix} i_{sD} & i_{sQ} & i_{mrd} & i_{mrq} \end{bmatrix}^T, \quad \boldsymbol{u} = \begin{bmatrix} u_{sD} & u_{sQ} \end{bmatrix}^T \\ \boldsymbol{y} &= \begin{bmatrix} i_{sD} & i_{sQ} \end{bmatrix}^T \end{aligned} \tag{2}$$

$$\boldsymbol{A}(|\boldsymbol{i}_{mr}|, \omega_r) = \begin{bmatrix} -c_1 & 0 & c_3 & a_{21} T_r f_1 \omega_r \\ 0 & -c_1 & -a_{21} T_r f_1 \omega_r & c_3 \\ a_{22}^* & 0 & -a_{22}^* & -\omega_r \\ 0 & a_{22}^* & \omega_r & -a_{22}^* \end{bmatrix},$$

$$\boldsymbol{G} = \begin{bmatrix} f_1 & 0 \\ 0 & f_1 \\ 0 & 0 \\ 0 & 0 \end{bmatrix}, \quad \boldsymbol{C} = \begin{bmatrix} 1 & 0 & 0 & 0 \\ 0 & 1 & 0 & 0 \end{bmatrix}$$

$$\boldsymbol{f}(\boldsymbol{x}) = \begin{bmatrix} \dfrac{c_2}{i_{mrd}^2 + i_{mrq}^2}\left(2 i_{sQ}^2 i_{mrd} - i_{sD}^2 i_{mrd} - 3 i_{sD} i_{sQ} i_{mrq}\right) \\ \quad + \dfrac{c_3 - a_{21} f_1}{i_{mrd}^2 + i_{mrq}^2}\left(i_{sD} i_{mrq}^2 - i_{sQ} i_{mrd} i_{mrq}\right) \\ \dfrac{c_2}{i_{mrd}^2 + i_{mrq}^2}\left(2 i_{sD}^2 i_{mrq} - i_{sQ}^2 i_{mrq} - 3 i_{sD} i_{sQ} i_{mrd}\right) \\ \quad + \dfrac{c_3 - a_{21} f_1}{i_{mrd}^2 + i_{mrq}^2}\left(i_{sQ} i_{mrd}^2 - i_{sD} i_{mrd} i_{mrq}\right) \\ \quad \dfrac{c_2}{i_{mrd}^2 + i_{mrq}^2}\left(i_{sD} i_{mrq}^2 - i_{sQ} i_{mrd}\right) \\ \quad \dfrac{c_2}{i_{mrd}^2 + i_{mrq}^2}\left(i_{sQ} i_{mrd}^2 - i_{sD} i_{mrq}\right) \end{bmatrix}. \tag{3}$$

For the list of symbols, the reader can refer to Table I. $\boldsymbol{A}(|\boldsymbol{i}_{mr}|, \omega_r)$, $\boldsymbol{f}(\boldsymbol{x})$, $\boldsymbol{G}$, and $\boldsymbol{C}$ are defined in (3) and coefficients a_{11}^*, a_{12}^*, a_{21}^*, a_{22}^*, and f_1 in $\boldsymbol{A}$ are defined as

$$\begin{aligned} a_{11}^* &= \frac{R_s}{\sigma L_s} + \frac{1-\sigma}{\sigma T_r^*} \qquad a_{12}^* = \frac{1}{\sigma L_s T_r^*} \\ a_{21}^* &= L_s \frac{1-\sigma}{T_r^*} \qquad a_{22}^* = \frac{1}{T_r^*} \qquad f_1 = \frac{1}{\sigma L_s} \end{aligned} \tag{4}$$

while coefficients c_1, c_2, and c_3 in $\boldsymbol{f}$ are defined as

$$\begin{aligned} c_1 &= a_{11}^* + a_{12}^*(\Delta L - 2\Delta L^*) \qquad c_2 = a_{12}^* \Delta L^* \\ c_3 &= a_{21}^* f_1 + a_{12}^*(\Delta L - \Delta L^*) \end{aligned} \tag{5}$$

with

$$\Delta L = L - L_m, \;\; \Delta L^* = \frac{L_{\sigma r}^2}{L_r^2} \Delta L. \tag{6}$$

T_r^* and L are called modified rotor time constant and dynamic magnetizing inductance, respectively, and are defined as in [1]

$$T_r^* = T_r \frac{L}{L_m} \tag{7}$$

$$L = \frac{d|\boldsymbol{\Psi}_r|}{d|\boldsymbol{i}_{mr}|} = L_m + |\boldsymbol{i}_{mr}| \frac{dL_m}{d|\boldsymbol{i}_{mr}|}. \tag{8}$$

For the Nomenclature, please refer to Table I.

It is to be highlighted that the matrix $\boldsymbol{A}$ of the state representation presents an indirect dependence from $|\boldsymbol{i}_{mr}|$; such dependence is due to the fact that the coefficients of such a matrix depend on the inductance and leakage factor terms, which are assumed variable with $|\boldsymbol{i}_{mr}|$. Furthermore, the highly nonlinear term $\boldsymbol{f}(\boldsymbol{x})$, depends on $|\boldsymbol{i}_{mr}|$ as well. It is to be observed that, under the hypothesis of linear behavior of the machine from the magnetic point of view, the static and dynamic inductances become equal, $L = L_m$, and both of them are assumed constant and independent from $|\boldsymbol{i}_{mr}|$. This last consideration implies that $T_r^* = T_r$ and $\Delta L = \Delta L^* = 0$, therefore, $c_1 = a_{11}$, $c_2 = 0$, and $c_3 = a_{21} f_1$. Consequently matrix $\boldsymbol{A}$ becomes time-variant only with respect to the variations of the rotor speed ω_r and becomes equal to the corresponding one of the classic dynamic model of the IM. Finally, under the assumption of linear magnetic behavior $\boldsymbol{f}(\boldsymbol{x}) = 0$ since $c_2 = 0$ and $c_3 - a_{21} f_1 = 0$. Consequently, the model assumes the form of that in [4], adopted for deriving a full order observer.

However, the proposed model takes into account only the saturation of the main flux, considering the first spatial harmonic of the magnetomotive force. It neglects any other magnetic saliency, such as the rotor slotting effect [26], and particularly it neglects the modification of such kind of saliency with the presence of the high-frequency signal injection [27].

The variation of the magnetic parameters of the IM, meaning the inductance and the leakage factor terms as well as the magnetizing curve, has been analyzed in details. In particular, the approach described in the following lies on an identification procedure based on experimental input–output data.

TABLE II
RATED DATA OF THE MOTOR

Rated power	2.2 kW	Rated speed	1425 r/min
Rated voltage	380 V	Rated torque	14.9 N·m
Rated frequency	50 Hz	Pole pairs	2
$\cos\phi$	0.75	Inertia moment	0.0067 kg· m^2

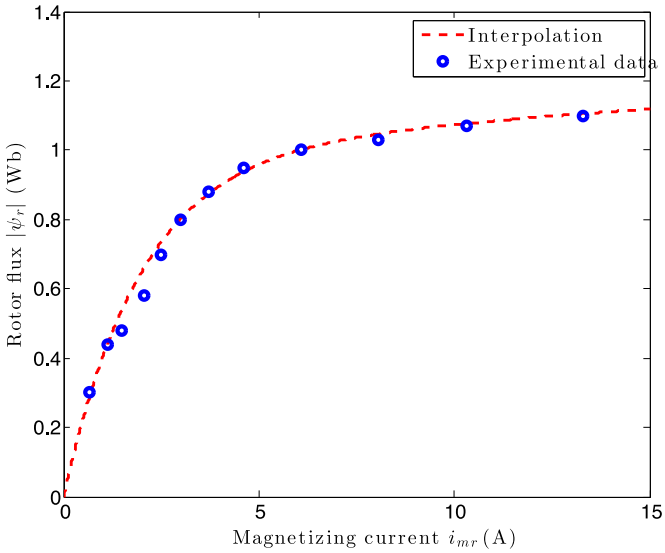

Fig. 1. Magnetizing curve of the IM.

A. Dependence of the Magnetic Parameters from the Rotor Magnetizing Current

Several important considerations must be made regarding the variation of the magnetic parameters of the IM from $|\boldsymbol{i}_{mr}|$, defining the magnetic working point on the IM magnetic characteristic. Since, as already pointed out above, the proposed nonlinear observer is based on the dynamic model of the IM including the magnetic saturation, implying the variation of its magnetic parameters with $|\boldsymbol{i}_{mr}|$, a suitable parameter estimation (identification) technique is to adopted [28].

As for the identification technique, the proposed in [28] has been used here, where, however, a completely different interpolation method has been considered.

As a matter of fact it is easily observable that, if the polynomial interpolation were adopted, above certain values of $|\boldsymbol{i}_{mr}|$, the amplitude of some parameters of machine (i.e., $|\boldsymbol{\Psi}_r|$, L_m, L_s, etc.) would assume an infinite value, with consequent incorrect working of the observer. To come up with this problem, specific analytical functions have been chosen to describe the variation of the inductances and leakage factor with the rotor magnetizing current. Consequently, a specific identification technique based on function interpolation has been derived, in order to overcome any numerical problem occurring above certain values of $|\boldsymbol{i}_{mr}|$. As a result, the experimental data can be better fitted with respect to [28]. As for the IM under test in this paper, (rated data are provided in Table II), Fig. 1 shows the magnetizing curve, expressing the relationship between the amplitude of the rotor flux linkage $|\boldsymbol{\Psi}_r|$ and the amplitude of the rotor magnetizing current $|\boldsymbol{i}_{mr}|$. The shape of the curve represented in Fig. 1 have suggested its representation as the sum of an exponential function with a linear one, as follows:

$$|\boldsymbol{\Psi}_r| = \alpha\left(1 - e^{-\beta|\boldsymbol{i}_{mr}|}\right) + \gamma|\boldsymbol{i}_{mr}|. \tag{9}$$

The nonlinear function in (9) presents a dependence on three parameters, α, β, and γ whose values for the IM under test have been computed on the basis of an optimization technique based on the nonlinear least-squares. In particular the starting point for determining the parameters α, β, and γ is the experimental determination of a set of points of the magnetic characteristic, i.e., the set of couples $\left(|\boldsymbol{i}_{mr}|_j,\ |\boldsymbol{\Psi}_r|_j\right)$, $j = 1, \ldots, N$, of the magnetic characteristics, obtained as described in [28]. In Fig. 1, the circles represent these points. Then, the determination of the above parameters is carried out using a curve fitting procedure, i.e., by means of formulation of a minimization problem whose performance index is the sum of the square differences between the experimental rotor flux and that computed using (9), for each value of magnetizing current belonging to the set of experimental data. The solution of the above problem is obtained by means of an optimization technique based on the nonlinear least-squares [29].

Such a nonlinear regression provided the following values: $\alpha = 0.98$, $\beta = 0.47$, and $\gamma = 0.01$. The correspondent interpolating curve is shown in dashed red in Fig. 1.

It is interesting to note that the coefficients α, β, and γ besides parameterizing the function describing the magnetizing curve of the IM, present a precise physical meaning. Such a physical meaning even permits to have a good feeling of their correct values, as obtained from the identification process. As a matter of fact, it must be considered that $\lim_{|\boldsymbol{i}_{mr}|\to 0} L_m = \alpha\beta + \gamma$ and $\lim_{|\boldsymbol{i}_{mr}|\to\infty} L_m = \gamma$; as a result γ can be interpreted as the magnetizing inductance when the IM is fully saturated, and the relation $\alpha\beta + \gamma$ as the tangent of the magnetizing curve for $|\boldsymbol{i}_{mr}| = 0$, representing the residual magnetization of the iron core. Looking at (9), it is absolutely reasonable above choosing α equal to the rated rotor flux amplitude. All the considerations provide a procedure that is alternative to the optimization one for obtaining the interpolating curve.

On the basis of (9), the analytical expression of L_m is obtained as

$$L_m = \frac{|\boldsymbol{\Psi}_r|}{|\boldsymbol{i}_{mr}|} = \alpha\frac{\left(1 - e^{-\beta|\boldsymbol{i}_{mr}|}\right)}{|\boldsymbol{i}_{mr}|} + \gamma. \tag{10}$$

After substituting the expression of L_m in (10) in (8), the expression L can be analytically inferred

$$L = \alpha\beta e^{-\beta|\boldsymbol{i}_{mr}|} + \gamma. \tag{11}$$

On the basis of such an approach, the analytical functions expressing the relationships with $|\boldsymbol{i}_{mr}|$ of all inductance and leakage factor terms can be deduced. As stated above, the only underlined simplifying assumption in the adopted model is that the stator, the rotor, and the global leakage inductances are assumed constant and, thus, independent from the magnetic saturation of the iron core (no dependence from $|\boldsymbol{i}_{mr}|$). Once the expression of L_m is assumed known from (10) and once the global leakage inductance is assumed known, as constant,

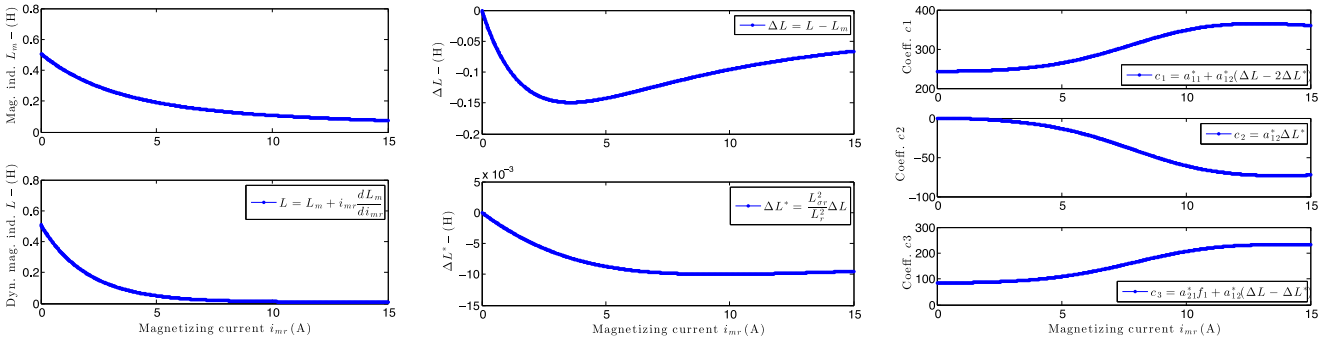

Fig. 2. (a) Magnetizing inductance L_m and dynamic magnetizing inductance L curves. (b) Curves of ΔL and ΔL^*. (c) Curves of the coefficients of the model c_1, c_2, and c_3.

measured on the basis of the locked rotor test, the expressions of all leakage factor with $|\boldsymbol{i}_{mr}|$ can be obtained.

Fig. 2(a) exhibits the relationships between L_m and L with $|\boldsymbol{i}_{mr}|$, respectively, whereas in Fig. 2(b) and (c), the waveforms of ΔL, ΔL^*, c_1, c_2, and c_3 are plotted.

It can be noted that only the variation of the three-phase magnetizing inductance L_m with the rotor magnetizing current $|\boldsymbol{i}_{mr}|$ has been considered, by means of (10). Then using the estimated magnetizing characteristic, and the $L_m(i_{mr})$, the expression of L, ΔL, and ΔL^* are obtained using (11) and (6). All the other parameters have been derived, together with the waveforms of the coefficients c_1, c_2, and c_3, by means of (4), (5), and (7). Note that the waveforms of the coefficients L, ΔL, ΔL^*, c_1, c_2, and c_3 shown in Fig. 2 are not imposed, but they are derived by their analytical expressions, starting from the variation of the L_m with main flux. So only the main magnetizing characteristic of the IM, providing the relationship between the rotor magnetizing current and the rotor flux amplitude, has been experimentally retrieved. All the other related variations of the parameters have been analytically inferred.

III. Nonlinear Observer

A first manner to obtain a nonlinear observer is to reproduce the approach adopted in case linear observers, whose starting point is the construction of a suitable model of the plant (1) and drive it with the "residual"

$$\boldsymbol{e}_y = \boldsymbol{y} - \hat{\boldsymbol{y}} = \boldsymbol{y} - \boldsymbol{C}\hat{\boldsymbol{x}}. \tag{12}$$

In all the equations, the symbol " $\hat{}$ " connotes the estimated variables. The observer's equation, therefore, becomes

$$\dot{\hat{\boldsymbol{x}}} = \boldsymbol{A}(|\boldsymbol{i}_{mr}|, \omega_r)\hat{\boldsymbol{x}} + \boldsymbol{f}(\hat{\boldsymbol{x}}) + \boldsymbol{G}\boldsymbol{u} + \boldsymbol{K}\boldsymbol{e}_y \tag{13}$$

where $\boldsymbol{K}$ is a suitably chosen matrix.

Note that in the matrix $\boldsymbol{A}(|\boldsymbol{i}_{mr}|, \omega_r)$ the variation laws of the parameters with $|\boldsymbol{i}_{mr}|$ is intrinsically incorporated, due to the knowledge of these laws thanks to the analysis given in Section II; moreover, the speed is assumed as a known parameter because it is measured.

Taking inspiration from [20], the choice of $\boldsymbol{K}$ can be done through the use of Lyapunov's second method. Using this method, Thau [20] shows the following result:

Theorem 1: If $\boldsymbol{f}(\boldsymbol{x})$ satisfies the Lipschitz condition, i.e., if $\forall \boldsymbol{x}_1, \boldsymbol{x}_2$ in the state space there exists a positive constant l such that

$$||\boldsymbol{f}(\boldsymbol{x}_1) - \boldsymbol{f}(\boldsymbol{x}_2)|| \leq l||\boldsymbol{x}_1 - \boldsymbol{x}_2|| \tag{14}$$

and if there exist two positive definite matrices $\boldsymbol{P}$ and $\boldsymbol{Q}$, and a positive constant λ_0 such that the following inequality is satisfied:

$$\mathrm{He}\left\{\boldsymbol{P}(\hat{\boldsymbol{A}} - \boldsymbol{K}\boldsymbol{C})\right\} = -\boldsymbol{Q} \leq -\lambda_0 \boldsymbol{I} \tag{15}$$

the convergence of the estimation error is assured for

$$\frac{\lambda_0}{2l||\boldsymbol{P}||} > 1 \tag{16}$$

where l is the Lipschitz constant in (14).

Proof: This analysis is summarized in [30, Sec. II], for a general case. However, for the sake of completeness, the analysis for the specific case under study has been carried out.

In the case under study, it is easy to verify that $\boldsymbol{f}(\boldsymbol{x})$ satisfies the locally Lipschitz condition. Indeed, $\boldsymbol{f}(\boldsymbol{x})$ is always derivable and its Jacobian is always bounded for bounded state variables in the normal operation conditions: i.e., for magnetization current greater than zero. So $\boldsymbol{f}(\boldsymbol{x})$ is locally Lipschitz for all $\boldsymbol{x}$ such that $i_{mrd}^2 + i_{mrq}^2 > \epsilon$, where ϵ is an arbitrary positive constant. However, this constraint is coherent with the physical requirement that the machine can correctly work only if it is magnetized and, consequently, (14) is always satisfied for any proper working condition.

The observer associated to model (1) is the closed-loop model (13). The dynamics of the state observation error $\boldsymbol{e} = \boldsymbol{x} - \hat{\boldsymbol{x}}$, is given by

$$\dot{\boldsymbol{e}} = (\boldsymbol{A} - \boldsymbol{K}\boldsymbol{C})\boldsymbol{e} + \boldsymbol{f}(\boldsymbol{x}) - \boldsymbol{f}(\hat{\boldsymbol{x}}) \tag{17}$$

where $\boldsymbol{A} \equiv \boldsymbol{A}(|\boldsymbol{i}_{mr}|, \omega_r)$. Assuming that $\boldsymbol{f}(\boldsymbol{x})$ is Lipschitz in a region of the state space $\mathscr{M}$, which includes all the possible admissible states and their estimates, we have

$$||\boldsymbol{f}(\boldsymbol{x}) - \boldsymbol{f}(\hat{\boldsymbol{x}})|| \leq l||\boldsymbol{x} - \hat{\boldsymbol{x}}|| \quad \forall \boldsymbol{x}, \hat{\boldsymbol{x}} \in \mathscr{M}. \tag{18}$$

By choosing as candidate Lyapunov function

$$V(\boldsymbol{e}) = \boldsymbol{e}^T \boldsymbol{P}\boldsymbol{e} \tag{19}$$

with $\boldsymbol{P}$ symmetric and positive definite, and computing its derivative $\dot{V}(\boldsymbol{e})$, it is obtained

$$\dot{V}(\boldsymbol{e}) = \boldsymbol{e}^T \left((\boldsymbol{A} - \boldsymbol{KC})^T \boldsymbol{P} + \boldsymbol{P}(\boldsymbol{A} - \boldsymbol{KC}) \right) \boldsymbol{e} + 2\boldsymbol{e}^T \boldsymbol{P} \left(\boldsymbol{f}(\boldsymbol{x}) - \boldsymbol{f}(\hat{\boldsymbol{x}}) \right). \tag{20}$$

If conditions (14) and (15) hold, (20) becomes

$$\dot{V}(\boldsymbol{e}) \leq -\left(\lambda_0 - 2l||\boldsymbol{P}||\right) ||\boldsymbol{e}||^2 \tag{21}$$

which implies that $\dot{V}(\boldsymbol{e}) < 0$ if $\lambda_0 > 2l||\boldsymbol{P}||$, i.e., if (16) holds.

With reference to the dynamics of the observation error, the previous analysis allows to conclude that the observation error converges to zero exponentially, with a rate which can be *a priori* fixed. In fact, (21) can be written as

$$\dot{V}(\boldsymbol{e}) \leq -\left(\lambda_0 - 2l||\boldsymbol{P}||\right) V(\boldsymbol{e}) \tag{22}$$

which is a differential inequality whose solution is

$$V(t) \leq e^{-(\lambda_0 - 2l||\boldsymbol{P}||)t} V(\boldsymbol{e}(0)). \tag{23}$$

So from (23) is evident that the observation error converges to zero exponentially with a rate greater than to $\lambda_0 - 2l||\boldsymbol{P}||$.

In order to obtain the gain matrix $\boldsymbol{K}$ such that conditions (15) and (16) are satisfied, the following theorem can be considered.

Theorem 2: Consider a matrix

$$\boldsymbol{P} = \begin{bmatrix} p_{11} & p_{12} \\ p_{21} & p_{22} \end{bmatrix} \otimes \boldsymbol{I}_2 = \begin{bmatrix} 1 & \frac{c_3}{(1+\chi)a_{22}^*} \\ \frac{c_3}{(1+\chi)a_{22}^*} & \frac{c_3^2}{(1+\chi){a_{22}^*}^2} + \chi \end{bmatrix} \otimes \boldsymbol{I}_2 = \bar{\boldsymbol{P}} \otimes \boldsymbol{I}_2 \tag{24}$$

where χ is a positive constant, and consider a gain $\boldsymbol{K}$ as

$$\boldsymbol{K} = \begin{bmatrix} k_1 & k_2 \end{bmatrix}^T \otimes \boldsymbol{I}_2 + \begin{bmatrix} 0 & k_\omega \end{bmatrix}^T \otimes \boldsymbol{J}_2 \tag{25}$$

with

$$\begin{aligned} k_1 &= \chi a_{22}^* - c_1 \\ k_2 &= a_{22}^* \\ k_\omega &= \frac{a_{21} T_r f_1 p_{11} - p_{12}}{p_{22}} \omega_r \end{aligned} \tag{26}$$

then conditions (15) and (16) are satisfied with $\lambda_0 = 2\chi a_{22}^*$, for any value of the rotor speed and of the magnetizing current.

Proof: Matrix $\boldsymbol{P}$ is symmetric and positive definite, indeed, it is easy to verify that $c_3 > 0$ [as also confirmed from Fig. 2(c)] and $a_{22}^* > 0$ for all values of the magnetizing current, so the coefficient $p_{22} > 0$ if $\chi > 0$; moreover, for the property of the Kronecker product (i.e., $\det(\boldsymbol{E}_n \otimes \boldsymbol{F}_q) = (\det(\boldsymbol{E}))^q (\det(\boldsymbol{F}))^n$), we have

$$\det(\boldsymbol{P}) = \left(\det(\bar{\boldsymbol{P}})\right)^2 \left(\det(\boldsymbol{I}_2)\right)^2 > 0 \qquad \forall \chi. \tag{27}$$

Noting that matrix $\boldsymbol{A}$ can be written as

$$\boldsymbol{A} = \begin{bmatrix} -c_1 & c_3 \\ a_{22}^* & -a_{22}^* \end{bmatrix} \otimes \boldsymbol{I}_2 + \begin{bmatrix} 0 & -a_{21} T_r f_1 \omega_r \\ 0 & \omega_r \end{bmatrix} \otimes \boldsymbol{J}_2 \tag{28}$$

fixing $\boldsymbol{K}$ as in (25), we can take advantage from the mixed-product property of the Kronecker product (i.e., $(\boldsymbol{E} \otimes \boldsymbol{F})(\boldsymbol{M} \otimes \boldsymbol{N}) = \boldsymbol{EM} \otimes \boldsymbol{FN}$) in order to compute $\mathrm{He}\{\boldsymbol{P}(\hat{\boldsymbol{A}} - \boldsymbol{KC})\}$. Indeed, we have that

$$\mathrm{He}\left\{\boldsymbol{P}(\hat{\boldsymbol{A}} - \boldsymbol{KC})\right\} = \mathrm{He}\left\{ \left(\bar{\boldsymbol{P}} \begin{bmatrix} -c_1 - k_1 & c_3 \\ a_{22}^* - k_2 & -a_{22}^* \end{bmatrix} \right) \otimes \boldsymbol{I}_2 + \left(\bar{\boldsymbol{P}} \begin{bmatrix} 0 & -a_{21} T_r f_1 \omega_r \\ -\frac{a_{21} T_r f_1 p_{11} - p_{12}}{p_{22}} \omega_r & \omega_r \end{bmatrix} \right) \otimes \boldsymbol{J}_2 \right\}. \tag{29}$$

In (29), it is easy to verify that the product

$$\bar{\boldsymbol{P}} \begin{bmatrix} 0 & -a_{21} T_r f_1 \omega_r \\ -\frac{a_{21} T_r f_1 p_{11} - p_{12}}{p_{22}} \omega_r & \omega_r \end{bmatrix}$$

is a symmetric matrix for each value of the parameters and of the speed ω_r. This means, for the property of the Kronecker product, that

$$\left(\bar{\boldsymbol{P}} \begin{bmatrix} 0 & -a_{21} T_r f_1 \omega_r \\ -\frac{a_{21} T_r f_1 p_{11} - p_{12}}{p_{22}} \omega_r & \omega_r \end{bmatrix} \right) \otimes \boldsymbol{J}_2$$

is skew-symmetric since $\boldsymbol{J}_2$ is skew-symmetric. Consequently,

$$\mathrm{He}\left\{ \left(\bar{\boldsymbol{P}} \begin{bmatrix} 0 & -a_{21} T_r f_1 \omega_r \\ -\frac{a_{21} T_r f_1 p_{11} - p_{12}}{p_{22}} \omega_r & \omega_r \end{bmatrix} \right) \otimes \boldsymbol{J}_2 \right\} = 0. \tag{30}$$

Note that (30) holds for each value of the parameters and of the speed ω_r. Now computing (29) under condition (30), we obtain

$$\begin{aligned} &\mathrm{He}\left\{\boldsymbol{P}(\hat{\boldsymbol{A}} - \boldsymbol{KC})\right\} \\ &= \left(\begin{bmatrix} 1 & \frac{c_3}{(1+\chi)a_{22}^*} \\ \frac{c_3}{(1+\chi)a_{22}^*} & \frac{c_3^2}{(1+\chi){a_{22}^*}^2} + \chi \end{bmatrix} \begin{bmatrix} -c_1 - k_1 & c_3 \\ a_{22}^* - k_2 & -a_{22}^* \end{bmatrix} \right. \\ &\quad \left. + \begin{bmatrix} -c_1 - k_1 & c_3 \\ a_{22}^* - k_2 & -a_{22}^* \end{bmatrix}^T \begin{bmatrix} 1 & \frac{c_3}{(1+\chi)a_{22}^*} \\ \frac{c_3}{(1+\chi)a_{22}^*} & \frac{c_3^2}{(1+\chi){a_{22}^*}^2} + \chi \end{bmatrix} \right) \otimes \boldsymbol{I}_2 \\ &= \begin{bmatrix} -2\left(c_1 + k_1 - \frac{(a_{22}^* - k_2)c_3}{(1+\chi)a_{22}^*}\right) & (\cdot) \\ \left(\frac{1+\chi}{a_{22}^*} + c_3\right)(a_{22}^* - k_2) - c_3 a_{22}^* (c_1 + k_1 - a_{22}^* \chi) & \\ -2\chi a_{22}^* & \end{bmatrix} \otimes \boldsymbol{I}_2. \end{aligned} \tag{31}$$

Choosing $k_2 = a_{22}^*$ and $k_1 = \chi a_{22}^* - c_1$, (31) simplifies in

$$\mathrm{He}\left\{\boldsymbol{P}(\hat{\boldsymbol{A}} - \boldsymbol{KC})\right\} = \begin{bmatrix} -2\chi a_{22}^* & 0 \\ 0 & -2\chi a_{22}^* \end{bmatrix} \otimes \boldsymbol{I}_2 = -2\chi a_{22}^* \boldsymbol{I}_4. \tag{32}$$

At the end, if the gain matrix is chosen such that $\begin{bmatrix} k_1 & k_2 \end{bmatrix}^T = \begin{bmatrix} \chi a_{22}^* - c_1 & a_{22}^* \end{bmatrix}^T$, then, for any $\chi > 0$, condition (15) is satisfied for $\lambda_0 = 2\chi a_{22}^*$.

Note that λ_0 can be chosen arbitrarily, since χ is arbitrary. It implies that there always exists χ such that (16) is satisfied.

Summarizing, in order to compute the gain $\boldsymbol{K}$ of the proposed observer, the value of χ have to be chosen; then, the value $\boldsymbol{P}$ in (24) is computed. By using the computed $\boldsymbol{P}$, the gain

components k_1, k_2, and k_ω are obtained by (26) and finally the gain $\boldsymbol{K}$ is computed as in (25). The corresponding speed of convergence of the observer can be evaluated using (23) considering that $\lambda_0 = 2\chi a_{22}^*$ as it is evident from the proof of Theorem 2.

Remark 1: The presented analysis shows that arbitrary global uniform exponential bounds can be imposed on the estimation error, regardless of the rotor speed. Moreover, it is shown that no bound neither on the rotor speed nor on the magnetizing current is required for the convergence of the estimation error. This bound on the estimation error is given in (23), and it is an arbitrary bound because it is related to the arbitrary choice of λ_0 as shown in the end of the proof of Theorem II. This aspect is particular important during the design phase of an observer, because the designer, beside to guarantee the convergence of the estimated variables in each operating condition, can choose the speed of convergence, and he can find, *a priori*, the correct tradeoff between filtering action and speed of convergence and in a systematic way. ⌟

Remark 2: It is useful to note that the observer gain $\boldsymbol{K}$ in (25) is composed of two parts, a symmetric part and a skew-symmetric part. Once the value of χ is chosen, the first part depends only on the magnetizing current, as it is evident from (26). The second skew-symmetric part, depends also from the speed, and from the choice of the Lyapunov matrix. In fact, once the value of χ is chosen, then, the matrix $\boldsymbol{P}$ is computed as in (24), and finally the value of k_ω is computed as in (26) by means of the speed. Beside the rigorous analysis presented in Theorem 2, this structure have an intuitive interpretation, indeed, the second part is necessary in order to remove the dependence of the dynamics from the speed, and then by means of the first part a suitably dynamics can be assigned, inducing a quadratically stable error dynamics with well-defined Lyapunov certificates. In fact, the observer gain given in (25) allows to have arbitrary global uniform exponential bounds on the estimation error, regardless of the rotor speed. Clearly, the error variables depend on ω_r and exhibit a peculiar time-varying transient, but the upper bound on their norm is a time-invariant function. A similar approach is shown in the recent work [13], but for a linear observer without takes into consideration the real magnetization characteristic of the machine. ⌟

Remark 3: A further important comment about the comparison between the presented approach and that one based on look-up tables needs to be given. In particular, the main difference between the proposed approach and that one based on look-up tables is not in the performance achieved, but it is in the design phase and the convergence guarantees that can be theoretically formalized with the presented approach. As it occurs for all the control/observation design based on gain scheduling methods (such as look-up tables), the stability of the overall control systems is not guaranteed or difficult to prove. Alternatively, the approach proposed in the paper gives, directly and in a closed form, the gains of the nonlinear observer, obtained so that the observation error not only converges to zero, but with an assigned convergence rate. Obviously, it is possible to use a look-up table, obtained by discretizing the waveforms of the observer gains versus the magnetizing current, in order to implement the proposed observer, and in particular, it is possible to substitute (25) with its graphical waveform defining a suitable look-up table. In this case, there are not differences and the same dynamic performances can be obtained between the proposed observer and an observer based on time varying gain defined with a look-up table. But it should be noted that the look-up table should be based on (25), and how to obtain the expression (25) is one of the main contributions of this paper. ⌟

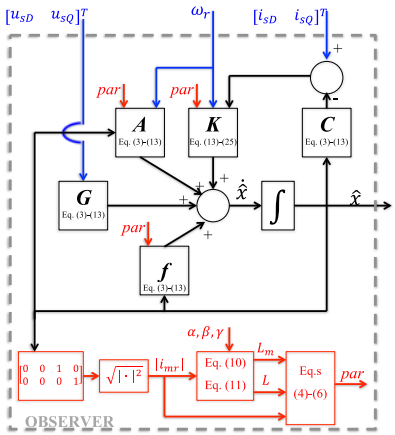

Fig. 3. Block diagram of the proposed observer.

With regard to the implementation of the proposed observer, a block diagram is shown in Fig. 3.

So, Theorem 2 represents a rigorous useful tool for designing the magnetizing current observer (13). Moreover, the shown result is particularly important because no bound on the rotor speed and on the magnetizing current is required, as far as the convergence of the estimation error is considered. For this reason, the proposed approach represents a general and useful tool for practitioners on this field, which want to design quickly a magnetizing current observer taking into account the magnetization characteristic.

IV. Experimental Setup

A laboratory setup has been constructed to experimentally test the behavior of the proposed nonlinear observer. The IM under study is a 2.2-kW IM SEIMEC model HF 100LA 4 B5, equipped with an incremental encoder. The adopted test setup is composed of the following:

1) a three-phase IM of rated power equal to 2.2 kW, whose rated data are provided in Table II;
2) a power converter consisting of a diode rectifier cascaded with a 7.5-kV· A three-phase IGBT voltage source inverter;
3) an electronic card with voltage sensors (model LEM LV 25-P) and current sensors (model LEM LA 55-P) for monitoring the stator phase voltages and currents and one voltage sensor (Model LEM CV3-1000) for monitoring the dc-link voltage;
4) a dSPACE card (DS1103) with a PowerPC 604e processor for fast floating-point calculation at 400 MHz, and a fixed-point DSP TMS320F240.

Fig. 4. Photo of the experimental setup.

The test setup is equipped also with a torque controlled PMSM model Emerson Unimotor FM mechanically coupled to the IM, to implement an active load for the IM. The torque is measured on the shaft by a torquemeter model Himmelstein 59003V(4-2)-N-F-N-L-K.

A photo of the employed test setup is shown in Fig. 4.

V. Simulation and Experimental Results

Numerical simulations have been performed in MATLAB-Simulink environment. With regard to simulations, as machine under test the dynamic model of the IM taking into consideration the magnetization characteristic has been adopted. It is basically the same dynamic model adopted for implementing the nonlinear observer. The simulated test has been performed twice, adopting the proposed nonlinear observer taking into consideration the magnetization characteristic, and adopting the classic FOLO that considers a linear magnetization characteristic. The classic FOLO has been tuned assuming constant electrical parameters of the IM, corresponding to the knee of the magnetization curve. With regard to the simulation test, a contemporary step variation of the IM reference speed, rotor flux amplitude, and load torque has been given, of the type: $\omega_{rref} = 20 \rightarrow 100$ rad/s, $|\mathbf{\Psi}_{rref}| = 0.2 \rightarrow 0.7$ Wb $t_L = 2 \rightarrow 10$ N· m.

With such a test, the drive works at different speeds with different load torques and rotor flux levels: such a working condition emulates the behavior of the drive in optimal efficiency conditions. To show the behavior of the observers, independently from the control action, both the nonlinear observer and the FOLO have been tested in parallel with respect to the control system, whereas the real flux has been feedback to close the flux control loop. Fig. 5 shows the real rotor flux amplitude and the estimated one as well as its phase position, obtained with both the observers, as well as the corresponding estimation errors. It can be seen that, approaching the rated flux of the IM, in correspondence to which the parameters of the FOLO have been tuned, both observers work correctly with the estimated fluxes correctly tracking the real ones. On the contrary, at rotor flux equal to 0.2 Wb, while the proposed nonlinear observer is able to correctly estimate the real flux, the classic FOLO

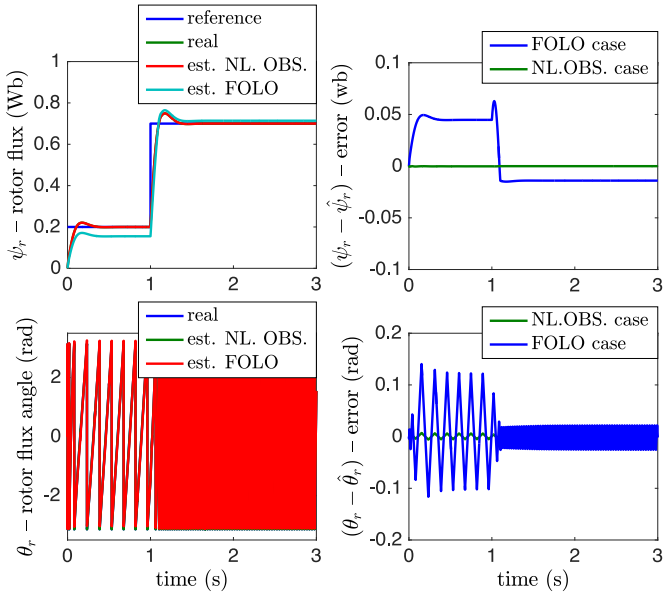

Fig. 5. Estimated and real rotor flux during a contemporary speed, flux, and torque step reference, $\omega_{rref} = 20 \rightarrow 100$ rad/s, $|\mathbf{\Psi}_{rref}| = 0.2 \rightarrow 0.7$ Wb $t_L = 2 \rightarrow 10$ (Simulation).

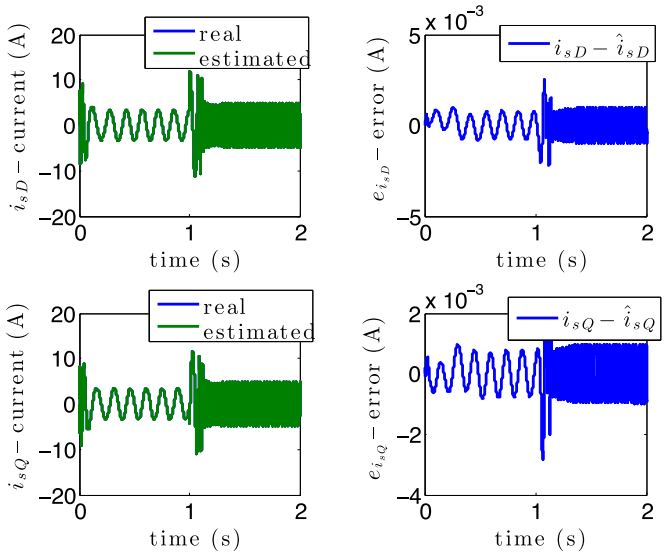

Fig. 6. Estimated and real i_{sD}-i_{sQ} stator current components with nonlinear observer during a contemporary speed, flux, and torque step reference, $\omega_{rref} = 20 \rightarrow 100$ rad/s, $|\mathbf{\Psi}_{rref}| = 0.2 \rightarrow 0.7$ Wb $t_L = 2 \rightarrow 10$ (Simulation).

presents a high-estimation error, equal to about 7% of the real flux.

Figs. 6 and 7 show, respectively, the real and estimated stator current components i_{sD} and i_{sQ} in the stator reference frame, as well as the instantaneous estimation error of both the observers. These figures clearly show that, while at the rated flux of the IM, in correspondence to which the parameters of the FOLO have been tuned, the observers tracking errors are very close to each other (as expected), for the lower value of the reference flux, the nonlinear observer significantly overcomes the FOLO in terms of estimation accuracy. In particular, it can be observed

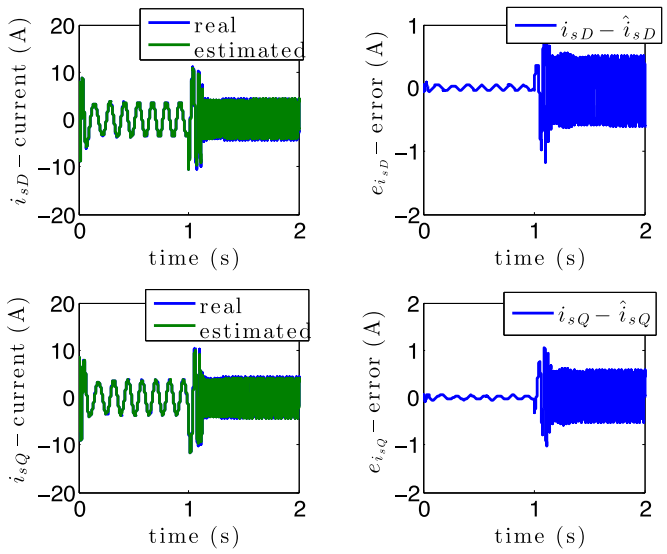

Fig. 7. Estimated and real i_{sD}-i_{sQ} stator current components with FOLO during a contemporary speed, flux, and torque step reference, $\omega_{rref} = 20 \rightarrow 100$ rad/s, $|\boldsymbol{\Psi}_{rref}| = 0.2 \rightarrow 0.7$ Wb $t_L = 2 \rightarrow 10$ (Simulation).

that the stator current estimation error is of the order 10^{-3} for the nonlinear observer, while it is of the order unity for the FOLO, confirming the goodness of the proposed approach. This is to be expected, since the nonlinear observer has embedded the knowledge of the magnetic working condition of the IM.

With regard to the experimental test, a set of contemporary step variation of the IM reference speed, rotor flux amplitude and load torque has been given, of the type: $\omega_{rref} = 20 \rightarrow 40 \rightarrow 60 \rightarrow 80$ rad/s, $|\boldsymbol{\Psi}_{rref}| = 0.2 \rightarrow 0.4 \rightarrow 0.6 \rightarrow 0.8$ Wb $t_L = 2 \rightarrow 4 \rightarrow 6 \rightarrow 8$ N· m. Fig. 8(a) shows the reference and measured speed under the above described test. Fig. 8(c) and (d) shows, respectively, the i_{sx}, i_{sy} measured and estimated stator current components in the rotor flux reference frame, as well as the instantaneous estimation error of both the observers. Such as in the numerical simulation case, the test has been performed twice, adopting the proposed nonlinear observer, and the FOLO. These figures confirm the simulation results and clearly show that, while approaching the rated flux of the IM, in correspondence to which the parameters of the FOLO have been tuned, the observers tracking errors are very close to each other (as expected), for low values of the reference flux (particularly 0.2 and 0.4 Wb), the nonlinear observer significantly overcomes the FOLO in terms of estimation accuracy. Correspondingly, Fig. 8(b) shows the waveform of the rotor magnetizing current amplitude, as obtained with both the observers, which is proportional to the rotor flux amplitude by $L_m(|\boldsymbol{i}_{mr}|)$. It can be observed that, while approaching the rated flux of the IM, the $|\boldsymbol{i}_{mr}|$ estimated by the two observers are very close to each other (as expected), for low values of the reference flux (particularly 0.2 and 0.4 Wb) they become quite different. In particular, at 0.2 Wb, the $|\boldsymbol{i}_{mr}|$ estimated by the nonlinear observer is much lower than that estimated with the FOLO, coherently with the fact that in the linear region of the magnetizing curve the static magnetizing inductance is much higher. Since there are no flux sensors embedded in the IM, no direct comparison could be made between the estimated and the measured value of the rotor flux. Nevertheless, an indirect confirmation of the accuracy of the flux estimation has been performed here comparing, with both the observers, the measured torque on the IM shaft (with the above described torque-meter) with the estimated torque. The torque has been estimated, with both observers, on the basis of the torque equation. Since it depends on the estimated rotor flux and the measured stator current, the verification of the accuracy of the torque estimation is an indirect verification of the accuracy of the flux estimation. It should be borne in mind that, coherently with the adopted model of the two observers, the torque estimation based on the nonlinear observer takes into consideration the variable parameters, while that based on the FOLO assumes constant parameters. Fig. 8(e) and (f) shows the electromagnetic and load torques, respectively, estimated with both the observers and measured. It can be observed that, while approaching the rated flux of the IM, the torque errors are very close to each other (as expected), for low values of the reference flux (particularly 0.2 and 0.4 Wb), the nonlinear observer significantly overcomes the FOLO observer in terms of estimation accuracy. In particular, at 0.2 Wb the torque error becomes even about 25% with the FOLO, while it is almost null with the proposed nonlinear observer. This is an indirect experimental confirmation of the better accuracy achievable in the rotor flux estimation with the proposed observer. Finally, also the time-varying gain components of the proposed nonlinear observer are shown in Fig. 9. In particular, the waveforms of k_1, k_2, and k_ω in (26) are plotted, representing the components of the matrix $\boldsymbol{K}$ in (25).

In order to better highlight the differences between FOLO and the proposed observer, a further experimental test has been carried out to evaluate the estimation accuracy in deep saturation condition. Differently from the first test, in this second test, the machine has been operated at constant speed of 50 rad/s, and a contemporary step variation of the IM magnetizing current amplitude and load torque has been given, of the type: $|\boldsymbol{i}_{mrref}| = 2 \rightarrow 4 \rightarrow 5 \rightarrow 6$ A, and $t_L = 0 \rightarrow 4 \rightarrow 8 \rightarrow 12$ N· m. Figs. 10–13 show the waveform of the estimated rotor flux, and the measured and estimated load torque, obtained with both observers. The analysis of such figures permits to make the following considerations. The flux curve clearly highlight that, starting from the same values of measured stator currents, stator voltages (the reference signal are adopted) and speed, the FOLO estimates much bigger values of the rotor flux amplitude. In particular, the higher is the flux level, the higher is the difference between the estimation with both observers. This is an intrinsic characteristic of the nonlinear observer accounting for the magnetic saturation. As a matter of fact, when the machine works in deep magnetic saturation, the nonlinear observer estimated the real flux amplitude, which is limited by the saturation phenomenon, while the FOLO largely overestimates the flux amplitude (1.3 Wb versus 1 Wb). The correctness of the better flux estimation accuracy obtained with the proposed nonlinear observer is indirectly verified by observing the electromagnetic torque estimation. It can be seen that torque estimated on the basis of the rotor flux estimated with the nonlinear observer is

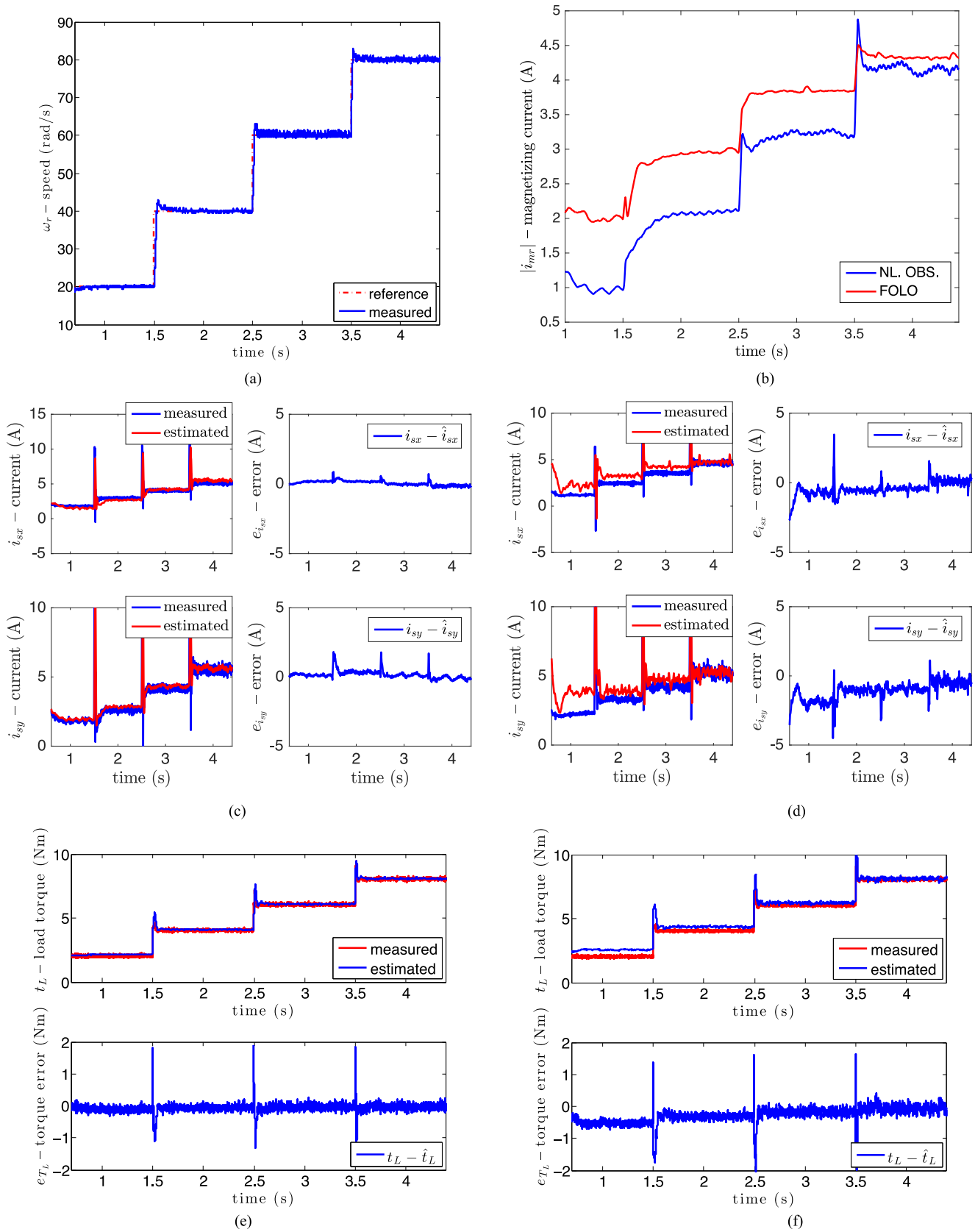

Fig. 8. Experimental results during a contemporary speed, torque, and flux step reference, $\omega_{r\,ref} = 20 \rightarrow 40 \rightarrow 60 \rightarrow 80$ rad/s, $|\boldsymbol{\Psi}_{r\,ref}| = 0.2 \rightarrow 0.4 \rightarrow 0.6 \rightarrow 0.8$ Wb $t_L = 2 \rightarrow 4 \rightarrow 6 \rightarrow 8$ N· m: (a) rotor speed; (b) rotor magnetizing current; (c) estimated and measured i_{sD}, i_{sQ} stator current components with nonlinear observer; (d) estimated and measured i_{sD}, i_{sQ} stator current components with FOLO; (e) estimated and measured electromagnetic torque with nonlinear observer; and (f) estimated and measured electromagnetic torque with FOLO.

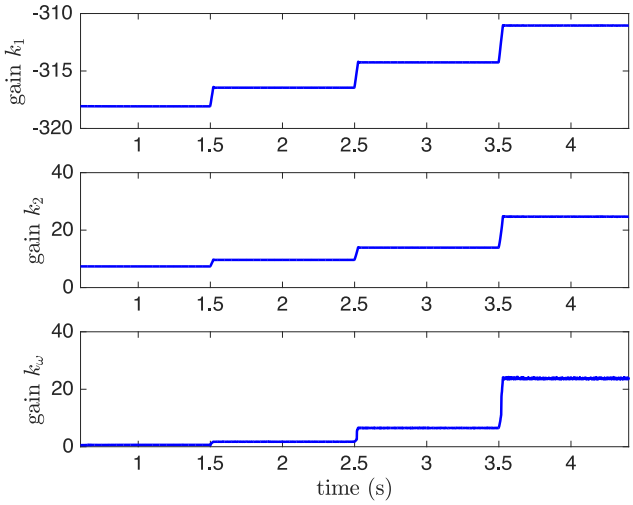

Fig. 9. k_1, k_2, and k_ω matrix gain components (25), for the experimental test in Fig. 8.

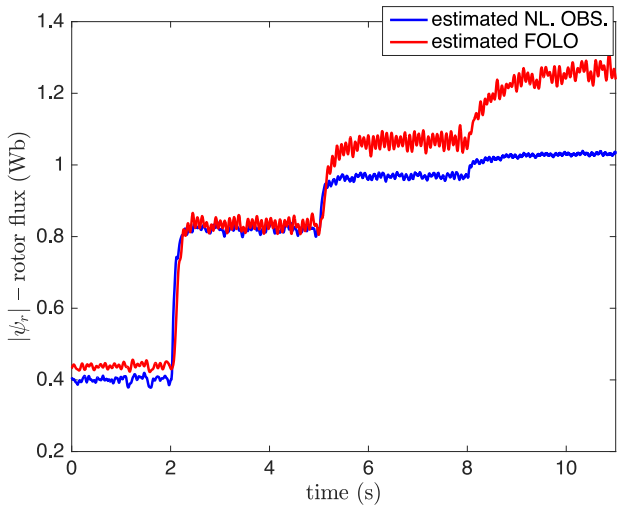

Fig. 10. Rotor flux estimates during an experimental test at constant speed of 50 rad/s, and with a contemporary step variation of the IM magnetizing current amplitude and load torque, of the type: $|\boldsymbol{i}_{mrref}| = 2 \rightarrow 4 \rightarrow 5 \rightarrow 6$ A, and $t_L = 0 \rightarrow 4 \rightarrow 8 \rightarrow 12$ N· m.

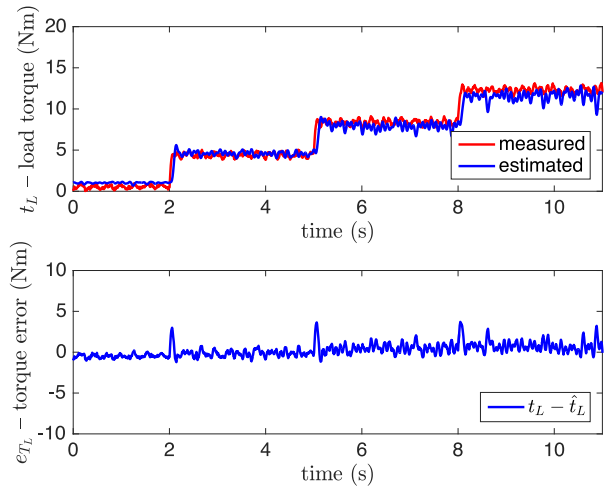

Fig. 11. Estimated and measured electromagnetic torque with nonlinear observer during an experimental test at constant speed of 50 rad/s, and with a contemporary step variation of the IM magnetizing current amplitude and load torque, of the type: $|\boldsymbol{i}_{mrref}| = 2 \rightarrow 4 \rightarrow 5 \rightarrow 6$ A, and $t_L = 0 \rightarrow 4 \rightarrow 8 \rightarrow 12$ N· m.

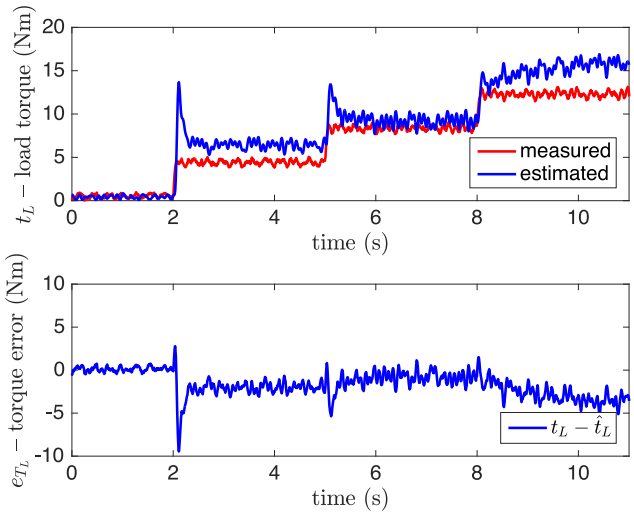

Fig. 12. Estimated and measured electromagnetic torque with FOLO during an experimental test at constant speed of 50 rad/s, and with a contemporary step variation of the IM magnetizing current amplitude and load torque, of the type $|\boldsymbol{i}_{mrref}| = 2 \rightarrow 4 \rightarrow 5 \rightarrow 6$ A, and $t_L = 0 \rightarrow 4 \rightarrow 8 \rightarrow 12$ N· m.

always much closer to the measured one than that estimated with the FOLO.

In details, to provide a metric of the increase of accuracy achievable in the rotor flux amplitude estimation, Figs. 14 and 15 show the percent flux estimation errors achieved experimentally with the proposed nonlinear observer and with the FOLO. These figures have been specifically inferred from the steady-state values of the torque errors in Figs. 8(e) and (f), 11, and 12. In particular, the flux error e_{ψ_r} has been computed starting from the torque error e_{t_e}, on the basis of the well-known expression of the IM electromagnetic torque $t_e = \frac{3}{2} p \frac{L_m}{L_r} |\boldsymbol{\psi}_r| \, i_{sy}$. On this basis, since i_{sy} is a measured quantity, which is not affected by any estimation error, if the knowledge of the IM parameters is assumed accurate, then, $e_{\psi_r} = \frac{2}{3p} \frac{L_r}{L_m} \frac{1}{i_{sy}} e_{t_e}$. Looking at Fig. 14, it can be noted that, while adopting the FOLO, the flux error increases from about 1% with the load torque of 8 N· m to about 20% with the load torque of 2 N· m, the corresponding flux error obtained with the proposed nonlinear observer ranges from less than 0.5% with the load torque of 8 N· m to less than 5% with the load torque of 2 N· m. Analogous considerations can be made with reference to Fig. 15, where the proposed nonlinear observer permits a flux estimation error always lower than 5%, whereas the FOLO presents an estimation error never lower than 10% and becoming close to 35% with the load torque of 2 N· m.

A. *Sensitivity Analysis*

With specific regard to the sensitivity analysis of the observer, such analysis has been carried out in numerical simulation by evaluating the rotor flux, and the stator current errors with re-

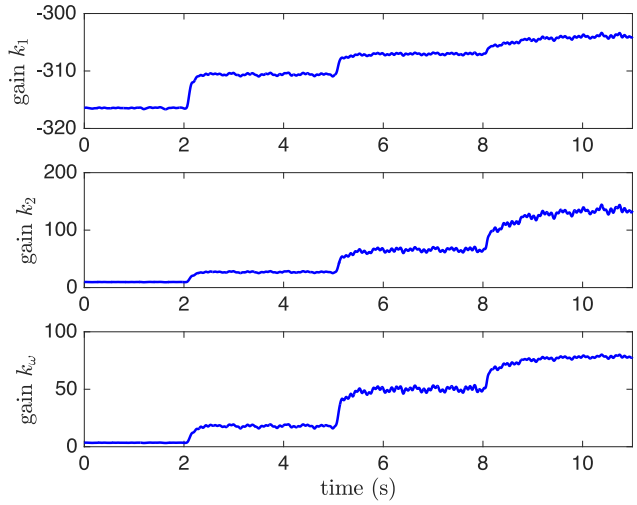

Fig. 13. k_1, k_2, and k_ω matrix gain components (25), for the experimental test in Figs. 10–12.

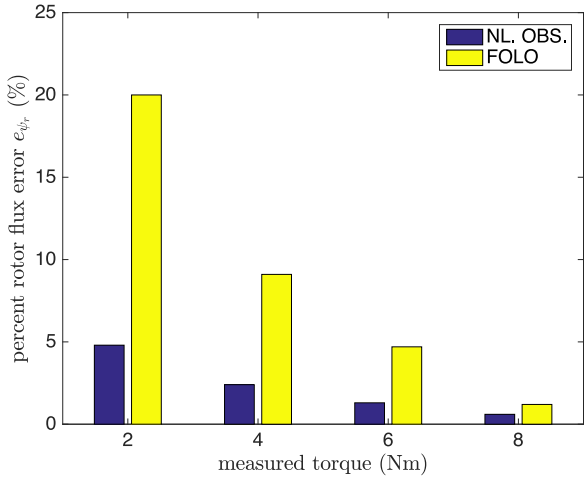

Fig. 14. Percent steady-state error of the flux estimation with the proposed nonlinear observer and with the FOLO related to the test in Fig. 8(e) and (f).

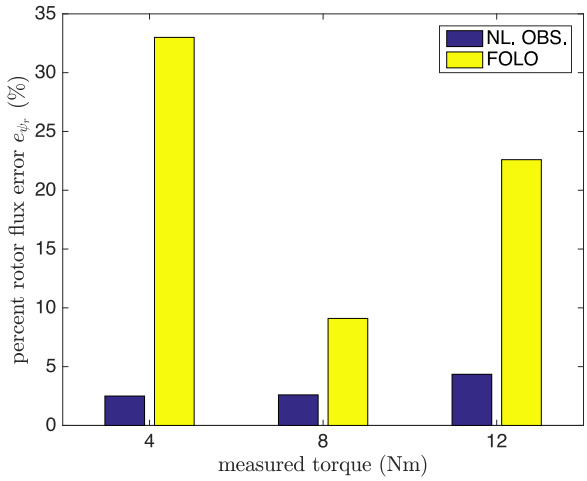

Fig. 15. Percent steady-state error of the flux estimation with the proposed nonlinear observer and with the FOLO related to the test in Fig. 11 and 12.

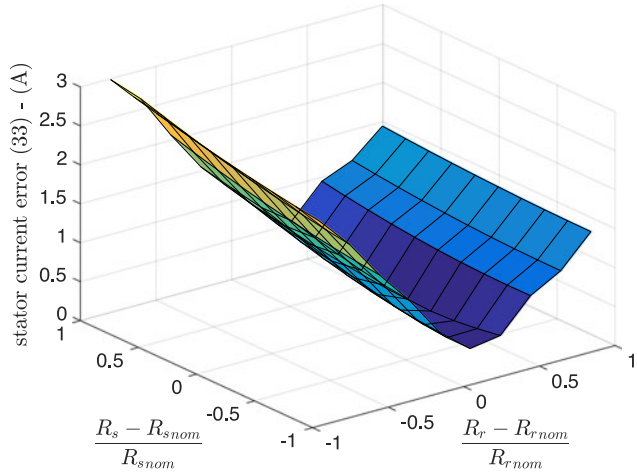

Fig. 16. Mean stator current errors computed as in (33) during a simulation test that reproduces the experimental test in Fig. 8.

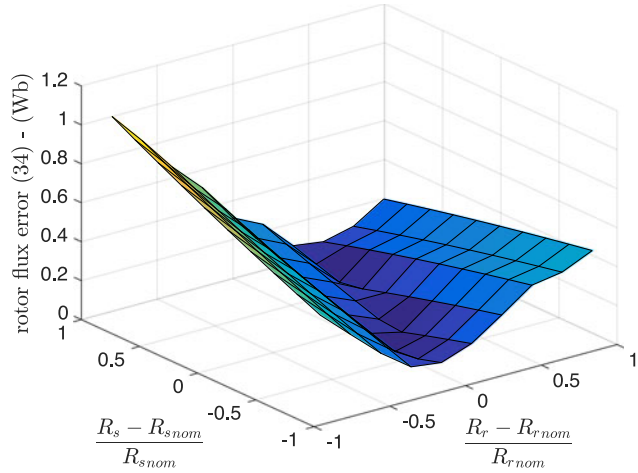

Fig. 17. Mean rotor flux errors computed as in (34) during a simulation test that reproduces the experimental test in Fig. 8.

spect to the variations of the stator and rotor resistances, which are the two main parameters that can change during the normal operation (heating, load, etc.). The test has been carried out by reproducing in simulation the experimental test shown in Fig. 8, and evaluating the mean errors computed as

$$e_{\boldsymbol{i}_s} = \sqrt{\left(i_{sx} - \hat{i}_{sx}\right)^2 + \left(i_{sy} - \hat{i}_{sy}\right)^2} \tag{33}$$

$$e_{\boldsymbol{\psi}_r} = \sqrt{\left(|\boldsymbol{\Psi}_r| - |\hat{\boldsymbol{\Psi}}_r|\right)^2}. \tag{34}$$

The results are shown in Figs. 16 and 17. Both resistances have been varied in the range between 20% and 200% of their rated values. The analysis of these figures shows that a mismatch of the stator resistance with respect to its rated value is less significant, in terms of both state components' estimations, than a corresponding mismatch of the rotor resistance with respect to its rated value. It is clearly visible that the error on both the stator current and the rotor flux linkage estimation is approximately independent from the stator resistance value, being strongly

dependent on the rotor resistance value. This consideration is particularly valid for the stator current estimation, while is less valid for the rotor flux estimation. This different sensibility is due to the fact that the stator resistance variation has a role on the stator equations, and since the stator current is the measurable part of the state given in input to the observer, the presence of a non-null gain of the observer permits to cover errors due to a wrong knowledge in the parameters that take place on these equations. On the contrary, an error on the rotor resistance gives a bigger contribute since it takes place on the rotor equations, and since the rotor flux cannot be measured, its accuracy in the estimation is related only on the accuracy of the model and its parameters. Obviously, the null errors are obtained for the nominal values $R_s = R_{s,nom} = 2.9\,\Omega$ and $R_r = R_{r,nom} = 1.55\,\Omega$. Moreover, the errors remain very small for an increment of the resistances with respect to their nominal values, while it becomes very high for big decrements of them.

VI. Conclusion

This paper proposes a nonlinear observer for IM drives that takes into consideration the saturation of the iron core. The nonlinear observer is based on an original formulation of the dynamic model of the IM taking into consideration the magnetization characteristic, suitably written in a state-space form and expressed in the stationary reference frame. It belongs to the category of the nonlinear observer characterized by a Lyapunov-based convergence analysis. The proposed nonlinear observer has been tested in numerical simulation and experimentally on a suitably developed test setup. Its behavior has been compared to that of a classic FOLO (which considers a linear magnetization characteristic) in variable flux working conditions, as well as the stator current components. Results clearly show the capability of such a nonlinear observer to correctly estimate the rotor flux amplitude and phase under flux varying conditions. Finally, a sensitivity analysis of the proposed observer versus the variations of both the stator and rotor resistances has been carried out.

References

[1] P. Vas, *Sensorless Vector and Direct Torque Control*. Oxford, U.K.: Oxford Univ. Press, 1998.

[2] W. Leonhard, *Control of Electrical Drives*. Berlin, Germany: Springer-Verlag, 2001.

[3] M. Cirrincione, M. Pucci, and G. Vitale, *Power Converters and AC Electrical Drives With Linear Neural Networks*. Boca Raton, FL, USA: CRC Press, 2012.

[4] H. Kubota, K. Matsuse, and T. Nakano, "DSP-based speed adaptive flux observer of induction motor," *IEEE Trans. Ind. Appl.*, vol. 29, no. 2, pp. 344–348, Mar./Apr. 1993.

[5] J. Maes and J. A. Melkebeek, "Speed-sensorless direct torque control of induction motors using an adaptive flux observer," *IEEE Trans. Ind. Appl.*, vol. 36, no. 3, pp. 778–785, May/Jun. 2000.

[6] L. Harnefors, "Design and analysis of general rotor-flux-oriented vector control systems," *IEEE Trans. Ind. Electron.*, vol. 48, no. 2, pp. 383–390, Apr. 2001.

[7] F. Alonge, F. D'Ippolito, G. Giardina, and T. Scaffidi, "Design and low-cost implementation of an optimally robust reduced-order rotor flux observer for induction motor control," *IEEE Trans. Ind. Electron.*, vol. 54, no. 6, pp. 3205–3216, Dec. 2007.

[8] Y.-R. Kim, S.-K. Sul, and M.-H. Park, "Speed sensorless vector control of induction motor using extended Kalman filter," *IEEE Trans. Ind. Appl.*, vol. 30, no. 5, pp. 1225–1233, Sep./Oct. 1994.

[9] F. Alonge, T. Cangemi, F. D'Ippolito, A. Fagiolini, and A. Sferlazza, "Convergence analysis of extended Kalman filter for sensorless control of induction motor," *IEEE Trans. Ind. Electron.*, vol. 62, no. 4, pp. 2341–2352, Apr. 2015.

[10] P. L. Jansen, R. D. Lorenz, and D. W. Novotny, "Observer-based direct field orientation: Analysis and comparison of alternative methods," *IEEE Trans. Ind. Appl.*, vol. 30, no. 4, pp. 945–953, Jul./Aug. 1994.

[11] P. L. Jansen and R. D. Lorenz, "A physically insightful approach to the design and accuracy assessment of flux observers for field oriented induction machine drives," *IEEE Trans. Ind. Appl.*, vol. 30, no. 1, pp. 101–110, Jan./Feb. 1994.

[12] G. C. Verghese and S. R. Sanders, "Observers for flux estimation in induction machines," *IEEE Trans. Ind. Electron.*, vol. 35, no. 1, pp. 85–94, Feb. 1988.

[13] A. Sferlazza and L. Zaccarian, "Linear flux observers for induction motors with quadratic Lyapunov certificates," in *Proc. 2016 IEEE 25th Int. Symp. Ind. Electron.*, IEEE, 2016, pp. 167–172.

[14] E. Levi, "Impact of cross-saturation on accuracy of saturated induction machine models," *IEEE Trans. Energy Convers.*, vol. 12, no. 3, pp. 211–216, Sep. 1997.

[15] X. Tu, L.-A. Dessaint, R. Champagne, and K. Al-Haddad, "Transient modeling of squirrel-cage induction machine considering air-gap flux saturation harmonics," *IEEE Trans. Ind. Electron.*, vol. 55, no. 7,xbrk pp. 2798–2809, Jul. 2008.

[16] C. Gerada, K. J. Bradley, M. Sumner, and P. Sewell, "Evaluation and modeling of cross saturation due to leakage flux in vector-controlled induction machines," *IEEE Trans. Ind. Appl.*, vol. 43, no. 3, pp. 694–702, May/Jun. 2007.

[17] R. T. Novotnak, J. Chiasson, and M. Bodson, "High-performance motion control of an induction motor with magnetic saturation," *IEEE Trans. Control Syst. Technol.*, vol. 7, no. 3, pp. 315–327, May 1999.

[18] A. Accetta, F. Alonge, M. Cirrincione, M. Pucci, and A. Sferlazza, "Feedback linearizing control of induction motor considering magnetic saturation effects," *IEEE Trans. Ind. Appl.*, vol. 52, no. 6, pp. 4843–4854, Nov./Dec. 2016.

[19] F. Alonge, M. Cirrincione, F. D'Ippolito, M. Pucci, and A. Sferlazza, "Robust active disturbance rejection control of induction motor systems based on additional sliding mode component," *IEEE Trans. Ind. Electron.*, 2017, to be published, doi: 10.1109/TIE.2017.2677298.

[20] F. Thau, "Observing the state of non-linear dynamic systems," *Int. J. Control*, vol. 17, no. 3, pp. 471–479, 1973.

[21] S. R. Kou, D. L. Elliott, and T. J. Tarn, "Exponential observers for nonlinear dynamic systems," *Inf. Control*, vol. 29, no. 3, pp. 204–216, 1975.

[22] G. Ciccarella, M. D. Mora, and A. Germani, "A Luenberger-like observer for nonlinear systems," *Int. J. Control*, vol. 57, no. 3, pp. 537–556, 1993.

[23] F. Alonge, M. Cirrincione, M. Pucci, and A. Sferlazza, "A nonlinear observer for rotor flux estimation considering magnetic saturation effects in induction motor drives," in *Proc. 2015 IEEE Energy Convers. Congr. Expo.*, IEEE, 2015, pp. 2892–2898.

[24] M. Hinkkanen, A.-K. Repo, M. Cederholm, and J. Luomi, "Small-signal modelling of saturated induction machines with closed or skewed rotor slots," in *Proc. 2007 IEEE 42nd IAS Annu. Meeting Ind. Appl. Conf.*, 2007, pp. 1200–1206.

[25] T. Tuovinen, M. Hinkkanen, and J. Luomi, "Modeling of saturation due to main and leakage flux interaction in induction machines," *IEEE Trans. Ind. Appl.*, vol. 46, no. 3, pp. 937–945, May/Jun. 2010.

[26] M. Cirrincione, M. Pucci, G. Cirrincione, and A. Miraoui, "Space-vector state model of induction machines including rotor slotting effects: Toward a new category of observers," *IEEE Trans. Ind. Appl.*, vol. 44, no. 6, pp. 1683–1692, Nov./Dec. 2008.

[27] J.-I. Ha, "Analysis of inherent magnetic position sensors in symmetric AC machines for zero or low speed sensorless drives," *IEEE Trans. Magn.*, vol. 44, no. 12, pp. 4689–4696, Dec. 2008.

[28] A. Accetta, F. Alonge, M. Cirrincione, M. Pucci, and A. Sferlazza, "Parameter identification of induction motor model by means of state space-vector model output error minimization," in *Proc. 2014 Int. Conf. Elect. Mach.*, IEEE, 2014, pp. 843–849.

[29] S. Van Huffel and J. Vandewalle, *The Total Least Squares Problem: Computational Aspects and Analysis*. Philadelphia, PA, USA: SIAM, 1991.

[30] W. S. Levine, *The Control Handbook: Control System Advanced Methods*. Boca Raton, FL, USA: CRC Press, 2011.

Francesco Alonge (M'02) was born in Agrigento, Italy, in 1946. He received the Laurea degree in electronic engineering from the University of Palermo, Palermo, Italy, in 1972.

Since then, he has been with the University of Palermo, where he is currently a Full Professor in automatic control in the Department of Systems and Control Engineering. His research interests include electrical drive control (including also linear and nonlinear observers, stochastic observers, parametric identification), robot control, parametric identification and control in power electronics, and unmanned aerial vehicle motion control in aeronautics.

Maurizio Cirrincione (M'03–SM'10) received the Laurea degree in electrical engineering from the Polytechnic University of Turin, Turin, Italy, in 1991, and the Ph.D. degree in electrical engineering from the University of Palermo, Palermo, Italy, in 1996.

Since 1996, he has been a Researcher with the I.S.S.I.A.-C.N.R. Section of Palermo (Institute on Intelligent Systems for Automation), Palermo. Since September 2005, he has been a Professor with the Université de Technologie de Belfort-Montbéliard, Belfort, France. Since April 2014, he has been the Head of the School of Engineering and Physics, University of the South Pacific, Suva, Fiji Islands. His current research interests include neural networks for modeling and control, system identification, intelligent control, power electronics, renewable energy systems, and electrical machines and drives.

Dr. Cirrincione received the 1997 E. R. Caianiello Prize for the Best Italian Ph.D. Thesis on neural networks.

Marcello Pucci (M'03–SM'11) received the Laurea and Ph.D. degrees in electrical engineering from the University of Palermo, Palermo, Italy, in 1997 and 2002, respectively.

In 2000, he was a Host Student with the Institute of Automatic Control, Technical University of Braunschweig, Braunschweig, Germany, working in the field of control of ac machines, with a grant from the German Academic Exchange Service. Since 2001, he has been with the Institute of Intelligent Systems for Automation, Section of Palermo, National Research Council of Italy, Palermo, where he is currently a Senior Researcher. His current research interests include electrical machines; control, diagnosis, and identification techniques of electrical drives; and intelligent control and power converters.

Dr. Pucci is an Associate Editor of the IEEE TRANSACTIONS ON INDUSTRIAL ELECTRONICS and the IEEE TRANSACTIONS ON INDUSTRY APPLICATIONS. He is a member of the Editorial Board of the *Journal of Electrical Systems*.

Antonino Sferlazza (S'12–M'15) was born in Palermo, Italy, in November 1987. He received the master's degree in automation engineering, and the Ph.D. degree in mathematics and automation from the University of Palermo, Palermo, in 2011 and 2015, respectively.

He is currently working as a Research Fellow in systems and control engineering with the Department of Energy, Information Engineering, and Mathematical Models, University of Palermo. His research interests include the development of feedback control algorithms for nonlinear dynamical systems, optimization techniques, estimation of stochastic dynamical systems, and applications of control of electrical drives, power converters, and mechanical systems.